2024 European Control Conference (ECC)
June 25-28, 2024. Stockholm, Sweden

Hybrid Optimal Control for an Active Mechanical Motion Rectifier for Wave Energy Converters via Separation Principle

Pedro Fornaro, John V. Ringwood

Abstract— **The wave energy field is characterised by its continuous growth and development in research and technology. Over recent decades, different application issues have hindered the worldwide implementation of wave energy devices, and only a few have reached the commercialisation stage. Some of these inherent challenges have driven the creation of innovative wave energy system designs. In particular, active mechanical motion rectification (AMMR) is a novel proposal to rectify the energy flux in wave energy devices. The objective of active rectification is twofold. On the one hand, it increases the overall system efficiency by achieving a higher average output velocity in the generator. On the other hand, the AMMR introduces a new variable in the control design: A switching law to connect and disconnect the generator from the wave capture structure. Thus, the control design possesses two degrees of freedom, significantly increasing the complexity of the energy-maximising power take-off control problem.**

In this paper, the problem of designing an optimal control philosophy for an AMMR-based wave capture system is addressed. The problem is solved by proving that, a separation principle applies, and that the optimal control solution over a fixed interval, is independent of the optimal switching sequence selection. To illustrate the utility of the analytical results, a numerical example for a flap-type wave energy converter, utilising an AMMR-based power take-off, is presented.

I. Introduction

In an international context, in which sustainability is relentlessly pursued to achieve the goal of net zero CO_2 emissions, wave energy will play a crucial role [1] [2]. The rationale behind this is simple. In essence, wave energy is capable of increasing the reliability of the currently available mix of renewable energy sources, by increasing the diversity and predictability of generated energy, while also reducing the need for energy storage systems [3].

While theoretically promising, with potential for high conversion efficiencies and substantial power output, the field performance of wave energy converters (WEC) is far less impressive. Achieving efficient wave-to-wire energy conversion necessitates extensive research developments in a variety of areas. This encompasses developments of wave capture body (WCB) structures, to convert the oscillating irregular wave energy into mechanical energy, power take-off (PTO) mechanisms, to convert mechanical energy into electricity, and advanced control strategies, to adapt the device to irregular wave excitations and maximise power extraction [4]. In these areas, interdisciplinary research plays a key role in improving the efficiency of current systems and innovating new devices, capable of achieving worldwide commercialization.

Regarding the typically employed PTOs, because wave energy is concentrated at low frequencies with time-varying velocities, efficient conversion becomes extremely difficult and limits the options for cost-effective PTO systems. Aiming to increase the efficiency of linear rotary generators, an active mechanical motion rectifier (AMMR) has recently been proposed [5] [6] [7]. In this system, two one-way electromagnetic clutches are used to mechanically rectify the oscillatory motion, resulting in unidirectional motion at the AMMR output shaft (see illustrative Figure 1). In combination with a rotary generator and a flywheel, in [6] [7] preliminary experimental tests were conducted, showing that this novel PTO structure is capable of achieving significant improvements in wave-to-wire efficiency.

When compared with directly coupled PTO mechanisms, the AMMR-based WEC also possesses distinctive advantages. First, the selection of the commutation intervals allows a discrete-time active control law (to synchronise the excitation torque with the WCB velocity) to be designed, independently of the employed continuous-time control law for the generator. Second, and ideally, improving the generator efficiency by increasing its average rotational speed is also possible. These concepts were preliminarily evaluated in [5], employing only passive damping control for the generator. However, the control law at the discrete-time level, to obtain maximum power extraction based only on the connection (clutching) and disconnection (declutching) of the AMMR, remains to be designed.

In this work, the design of a hybrid optimal control algorithm, capable of maximising the power output for this system, is addressed. To that end, first, following the previous developments from [8] [9], the hybrid machine model is employed. Using the framework from [10] [11], it is proven that the algorithms to decide the continuous-time controller for the generator and discrete-time decision-making for the clutching and declutching of the AMMR, can be separately designed. Then, the hybrid optimal control maximises (mechanical) power extraction from the WCB, provided that E (defined in (1)) is also maximised.

$$E(t_f) = \int_{t_0}^{t_f} y(\varepsilon)\tau_u(\varepsilon)\mathrm{d}\varepsilon, \tag{1}$$

This work was possible thanks to the support of the National University of Maynooth, Science Foundation Ireland under grant number 21/US/3776, and of the University Nacional de La Plata, Argentina.

Pedro Fornaro is with the Centre for Ocean Energy Research, Department of Electronic Engineering, Maynooth University, Co. Kildare, Ireland, and with the Instituto LEICI, Fac. de Ingeniería/UNLP - CONICET, La Plata, Bs.As., Argentina, (email: pedro.fornaro@mu.ie).

John V. Ringwood is with the Centre for Ocean Energy Research, Department of Electronic Engineering, Maynooth University, Co. Kildare, Ireland (email: john.ringwood@mu.ie).

where $y(t)$ is the WCB velocity (assumed angular for this study), $\tau_u(t)$ is the control torque, and $E(t)$ is a cost function to be evaluated and maximised in specific intervals by a suitable selection of the control variables.

The remainder of the paper is structured as follows: In Section II, the employed AMMR-based WEC hybrid model is developed. Section III presents the hybrid optimal control problem, along with the formulation of alternative proposals. In Section IV, some numerical examples based on a flap-type WEC are presented. Lastly, Section V provides the concluding remarks.

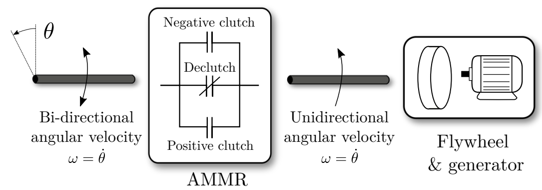

Fig. 1. Illustrative AMMR-based PTO scheme, conformed with the AMMR, a rotary generator and an interconnected flywheel.

II. Hybrid systems approach to AMMR-based WEC modelling

In this section, the hybrid model employed to represent the system dynamics is presented. To that end, the working principle of the AMMR is described, and, its connection with the hybrid framework, is established.

A. AMMR operating principle

The AMMR possesses a variety of functions, but the rectification of mechanical motion is its primary objective. Employing this mechanism, the output shaft of the generator rotates unidirectionally. If the AMMR clutches are disengaged before the velocity reaches zero, and re-engaged after the WCB velocity surpasses a predefined limit, then the generator efficiency can also be increased. Furthermore, with the inclusion of a flywheel in the system, is possible to increase the average rotational speed of the generator during the disengagement stages.

As illustrated in Figure 1, the AMMR possesses three distinctive operation modes. In the first operation mode, with the positive clutch engaged, the WCB is connected to the generator and flywheel through a mechanical drivetrain, and both input and output of the AMMR rotate in the same direction. In the second operation mode, the negative clutch is engaged and input and output of the AMMR rotate in opposite directions. In the third operation mode, both clutches are disengaged, with the generator and WCB decoupled.

In each one of the operation modes, the system dynamics vary. On the one hand, when the AMMR clutches are disengaged, the WCB is uncontrolled. On the other hand, when the AMMR clutches are engaged, the flywheel increases the system inertia, but also, a continuous-time control law may be applied, changing the system dynamics.

To visually represent the described system behaviour, a graph diagram is constructed (See Figure 2). In it, q represents the different discrete states (operation modes) of the system. With $q = 1$, the positive clutch is engaged; with $q = -1$ the negative clutch is engaged and, with $q = 0$, the clutches are disengaged. Also, the notation $f(q, \mathbf{x}, \tau_u)$ represents how the system dynamics are also dependent on the discrete state q, and the events that drive the system from one discrete state to another state are c^+, c^-, c^0, representing positive clutch engagement, negative clutch engagement, and disengagement, respectively.

B. Hybrid model of the AMMR-based WEC

Hybrid system models exhibit both continuous and discrete-time behaviour, and although there exist different modelling frameworks used to describe several classes of hybrid systems, in this work, the hybrid machine (HM) description is used. In this representation, the model is composed of an automaton to model discrete-time events, and a state space model to represent the evolution of the continuous-time variables.

Employing the HM description, the state space representation is parametrised as a function of the automaton discrete states q, which normally take values only within a known finite and non-empty set Q. As previously presented, for the current case, $Q : \{1,\, 0,\, -1\}$. Formally, in this paper, the HM is defined as:

$$\mathcal{HM} = (Q,\, \Sigma,\, \delta,\, q_i,\, V,\, D), \tag{2}$$

where $\Sigma : \{c^+,\, c^0,\, c^-\}$ is the set of possible events, $\delta : Q \times \Sigma \rightarrow Q$ determines the dynamics of the events at the discrete-time level, q_i is the initial discrete state, V is the set of continuous variables comprising control actions $\tau_u(t) \in \mathbb{R}^m$ and states $\mathbf{x} \in \mathbb{R}^n$, and $D : \{f(q, \mathbf{x}, \tau_u),\, q \in Q\}$ is the continuous time mapping from $Q \times \mathbb{R}^n \times \mathbb{R}^m \rightarrow \mathbb{R}^n$. It is also worth noting that, although the system dynamics might change for different states $q \in Q$, the states $\mathbf{x}$ are continuous, while the control action τ_u may be discontinuous.

To complete the model, in the remainder of this section, $f(q, \mathbf{x}, \tau_u)$ is obtained. To that end, the following assumptions (essential to develop a preliminary AMMR hybrid control strategy) regarding the AMMR and generator are made. First, the AMMR is considered ideal. This implies that the system is capable of instantly, and free of losses, connecting or disconnecting the generator from the WCB. Second, the

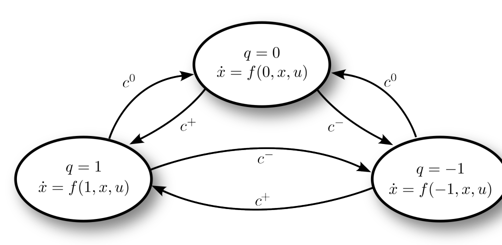

Fig. 2. Illustrative hybrid machine graph, considering the three AMMR discrete states and a strongly connected graph.

generator dynamics are neglected. Also, although, in general, $f(q, \mathbf{x}, \tau_u)$ may be nonlinear, for simplicity sake, particularly for Section IV, the analysis is focused on the commonly employed second-order linear model.

To derive $f(q, \mathbf{x}, \tau_u)$, it is firstly assumed that the clutches are engaged. Also, regardless of the employed WCB, the input to the AMMR is a one-degree-of-freedom bi-directional rotational motion, which is typically a pinion driven by a rack from a heaving buoy (straight rack) or oscillating wave surge converter (curved rack). Therefore, without loss of generality, $\theta(t)$ is defined as the AMMR angular position. Employing the mentioned assumptions, the second-order state space model, with the clutches engaged, is [12]:

$$J_T\,\ddot{\theta}(t) = -B_r\dot{\theta}(t) - K\theta(t) + \tau_{ex}(t) + q\tau_u(t), \tag{3a}$$

$$y(t) = \dot{\theta}(t), \tag{3b}$$

where each term is referred to the AMMR input shaft: J_T is the sum of the WCB, generator and flywheel inertia, B_r is the WCB damping, $\tau_u(t)$ is the control action and $\tau_e(t)$ is the excitation torque provided by the reciprocating motion of waves. Observe that, due to q, the sign premultiplying $\tau_u(t)$ is positive (negative) with the positive (negative) clutch engaged.

On the other hand, when the clutches are both disengaged, the generator torque and flywheel effects must not be considered. Therefore, the dynamics of the disengaged system are given by:

$$J_P\,\ddot{\theta}(t) = -B_r\dot{\theta}(t) - K\theta(t) + \tau_{ex}(t) \tag{4a}$$

$$y(t) = \dot{\theta}(t), \tag{4b}$$

where the inertia J_P considers only the WCB inertia. Assuming that $\theta(t)$ is the angular displacement at the input shaft of the AMMR, and omitting the time argument, the unified dynamics of the system are given by:

$$\dot{\mathbf{x}} = \mathbf{A}_q\mathbf{x} + \mathbf{B}_q\tau_u = \tag{5a}$$

$$\begin{bmatrix}\dot{x}_1\\ \dot{x}_2\end{bmatrix} = \begin{bmatrix}0 & 1\\ \frac{-K}{J_q} & \frac{-B_r}{J_q}\end{bmatrix}\begin{bmatrix}x_1\\ x_2\end{bmatrix} + \begin{bmatrix}0\\ \frac{q}{J_q}\end{bmatrix}\tau_u + \begin{bmatrix}0\\ \frac{1}{J_q}\end{bmatrix}\tau_{ex}$$

$$y = \mathbf{C}_q\mathbf{x} = \begin{bmatrix}0 & 1\end{bmatrix}\begin{bmatrix}x_1\\ x_2\end{bmatrix}, \tag{5b}$$

where $[x_1\ x_2]^\intercal := [\theta\ \dot{\theta}]^\intercal$, and J_q is the system inertia represented as a function of the discrete states. For further details about the model please refer to [9] [12].

III. Hybrid optimal control

In this section, the hybrid control problem is formulated, and optimal and sub-optimal solutions are presented and discussed. First, it is important to recapitulate some concepts about HMs. Historically, HMs have been used to represent the dynamics of nested systems, in which the main goal is regulation and system stabilisation [13]. In the AMMR case, however, the system is driven through different discrete states. In general, a constant adaptation of the control law is required, since, the excitation torque needs to be tracked to achieve maximum power extraction (via synchronisation of the WCB velocity and applied excitation force) [14].

In this context, designing a hybrid control law requires obtaining the continuous-time control action τ_u, and a discrete-time sequence of events capable of maximising (1). To explicitly visualise how (1) is a function of both continuous and discrete control actions, is rewritten as:

$$\begin{aligned} E(t_f) &= \int_{t_0}^{t_f} y(\varepsilon)\tau_u(\varepsilon)\mathrm{d}\varepsilon = \\ \sum_{i=0}^{N-1} E_i(t_{i+1}) &= \sum_{i=0}^{N-1}\int_{t_i}^{t_{i+1}} y_q(\varepsilon)\tau_{u_q}(\varepsilon)\mathrm{d}\varepsilon, \end{aligned} \tag{6}$$

where N is the number of switches in $[0; t_f]$, the subindex q is used to explicitly denote the dependence with the discrete state q, and $E_i(t_{i+1})$ is defined as the *i-th* term of the summation. Note that infinite frequency switching is not considered in this work. Instead, only a finite number of switches within a period of the excitation torque is considered.

Maximising $E_i(t_{i+1})$, in (6), is equivalent to solving the classical finite-horizon optimal control problem. If $q = \pm 1$, then, τ_{u_q} can be designed. However, when $q = 0$, the clutches are disengaged and there is no control torque to be applied. Thus, the problem is reformulated as follows. Instead of considering maximising the PTO power output, the mechanical power *dissipated* by the WCB is considered. Then, by definition, $E_i(t_{i+1})$ is equivalent to:

$$E_i(t_{i+1}) = \int_{t_i}^{t_{i+1}} \tau_{ex}(\varepsilon)y_q(\varepsilon) - L(y_q(\varepsilon))\mathrm{d}\varepsilon, \tag{7}$$

where $L(y_q(t))$ represents the mechanical losses of the WCB. Observe that since (7) is a function of $y_q(t)$, the velocity that maximises $E_i(t_{i+1})$ is the theoretical system output when the optimal control action is used. Thus, this variation of the optimal control problem arrives at an optimal solution employing $y_q(t)$. Then, the continuous control action that guarantees $y_q := x_2$ is extracted from (5a).

Another implication of this formulation is that the effect of switching to maximise mechanical power in the WCB can be visualised. Specifically, even when it is not possible to extract mechanical power because $q = 0$ (and $\tau_{u_q} = 0$), the switching affects the mechanical power absorbed by the WCB. To visualise this, rewrite $E(t_f)$ as:

$$\begin{aligned} E(t_f) &= \int_{t_0}^{t_f} y(\varepsilon)\tau_u(\varepsilon)\mathrm{d}\varepsilon = \\ &\sum_{i=0}^{N-1}\int_{t_i}^{t_{i+1}} \tau_{ex}(\varepsilon)y_q(\varepsilon) - L(y_q(\varepsilon))\mathrm{d}\varepsilon. \end{aligned} \tag{8}$$

Thus, although $\tau_{u_q} = 0$ during the disengagement stage, the main goal of maximising mechanical output power is affected by both the selection of the switching intervals *and* the control law τ_{u_q}. If $q = 0$, then no continuous control action is applied, but mechanical power variation in the WCB is considered. Also, if $q \neq 0$, then the finite horizon optimal continuous-time control problem must be solved in each $t \in (t_i, t_{i+1})$. Employing the presented problem formulation, in the following section, the separation principle to solve the hybrid optimal control problem is introduced.

A. Separation principle

Maximising (8) requires obtaining the optimal discrete-time control action, i.e., the optimal switching sequence for the AMMR, including the commutation intervals, and the optimal continuous-time control action applied by the generator. To that end, the following lemma is presented.

Lemma 1: Considering that the dynamics of the WEC are described by (5), for the design of the hybrid optimal control for the AMMR-based WEC, the continuous-time control (generator torque) solution is independent of the discrete-time control (switching sequence).

Proof: The proof is made by obtaining the optimal continuous-time control action for a specific time interval $[t_i, t_{i+1}]$. To that end, customise (8) for the system in (5), and solve the optimal continuous-time control algorithm as follows. First, the cost function to maximise in the *i-th* interval is:

$$E_i(t_{i+1}) = \int_{t_i}^{t_{i+1}} \tau_{ex}(\varepsilon) y_q(\varepsilon) - B_r y_q^2(\varepsilon) \mathrm{d}\varepsilon. \tag{9}$$

Thus, trivially, the quadratic argument in (9) is maximum when $y_q = \tau_{ex}/2B$ (A standard result in wave energy control [1]). Then, replace y_q in (5a) (recall that $x_2 := y_q$), and the optimal control action:

$$\tau_u^{op} = \tau_{ex} + Kx_1 + B_r x_2 + \tfrac{J_q}{2B_r} d\tau_{ex}/dt, \tag{10}$$

is obtained. Therefore, τ_u^{op} is causal and, over a finite time interval, guarantees synchronisation of τ_{ex} with the WCB velocity and maximum mechanical energy extraction independently of the switching instances t_i, and t_{i+1}. ■

It can be also stated that, if a control (continuous for the generator or discrete for the switching law) is designed, then the other can be subsequently adjusted to achieve local maximum power extraction. For instance, with a predefined generator control law, the problem of maximising (8) reduces to finding the optimal switching intervals.

It is worth mentioning that including constraints in the definition of (8) is, for the time being, beyond the scope of this paper. Thus, Lemma 1 becomes useful to focus on preliminary theoretical developments for the design of a hybrid optimal control law for the AMMR. Furthermore, Lemma 1 has several implications from the point of view of control design:

- First, because selecting a continuous control action is independent of the employed switching law, the energy-maximising problem could be iteratively solved, assuming that one of the control structures (continuous or discrete time) is predefined.
- Second, assuming a fixed hybrid control structure, the effects of varying the flywheel inertia could be evaluated, which is essential to address the co-design of AMMR-based WECs.
- Third, this problem formulation permits establishing a simple methodology to analyse the results of varying the switching law, and its effects (benefits, differences, inconveniences) when compared with classical control structures for wave energy devices.

In the following subsections, three proposals to solve the AMMR-based WEC control problem are presented and analysed. To ease the presentation of the results, in the following subsections a second-order linear model, as in (5), is employed.

B. Continuous-time control: Sub-optimal proposal

A sub-optimal proposal may be formulated, predefining the switching law, and maximising (8) within every switching interval with $q = \pm 1$. With this proposal, because the switching law is fixed, the theoretical maximum power output may not be obtained. Then, the problem is reduced to obtaining a sub-optimal continuous-time control action. One reason to predefine the AMMR behaviour is to guarantee positive average velocity in the generator. Therefore, it is expected that fixing the switching law, may produce a high power output while increasing generator efficiency, and simplifying the controller design. The control structure for this system can be appreciated in Figure 3.a. In this case, assuming a second-order linear model, the solution of the optimal control τ_u^{op}, is the same as (10).

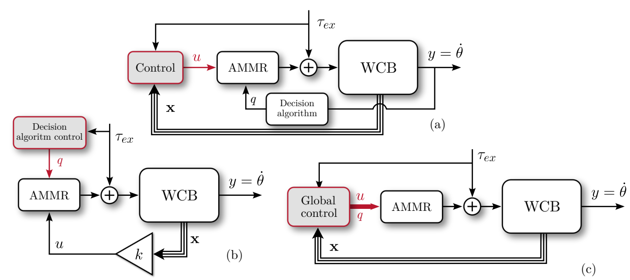

Fig. 3. Illustrative scheme of the control diagram. a) AMMR is controlled via a predefined switching law dependent on the WCB velocity. b) AMMR controlled via control from Subsection III-C. c) Global optimal hybrid control from Subsection III-D.

C. Discrete-time (switching) control: Suboptimal proposal

In this subsection, an algorithm to determine the optimal switching time for the AMMR, while the control law is fixed, is presented. First, it is essential to mention that, unlike the case in Subsection III-B, solving the optimal switching sequence requires further information on some system variables, including the excitation torque τ_{ex}, the continuous-time control algorithm, and the time interval $T = t_f - t_0$. Then, the problem reduces to evaluating which time instants t_i maximise $E(t_f)$ in (6).

The procedure for the selection of the switching control algorithm, presented in this paper (illustrated in Figure 3.b.), is summarised as follows:

1) Define the control structure employed in the controlled intervals. This sets the system dynamics (5).
2) Define the time horizon $T = t_f - t_0$.
3) Define the number (N) of switching points in T.
4) Compute the cost function $E(t_f) := E(t_{i+N})$ as a function of the switching intervals t_i.
5) Obtain the $[t_i, ..., t_{i+N}]$ vector that maximises $E(t_{i+N})$.

TABLE I
WCB PARAMETERS FOR THE EMPLOYED WAVE PERIOD.

Wave period [s]	J_T [Kgm^2]	J_P [Kgm^2]	B_r [Nms/rad]	K [Nm/rad]
2.4	89	77	75	285

It is worth noting that the procedure in 1-5 above, is independent of the employed control structure. Thus, it is possible to obtain switching sequences that maximise power output with predefined controllers. Therefore, higher-order WCB models could also be employed, without considerably increasing the complexity of the control problem.

D. Global optimal control structure

The global hybrid optimal control structure, results from applying an optimal control strategy (Subsection III-B) during the engagement, and simultaneously, the procedure from Subsection III-C to define the switching intervals. This proposal is illustrated in Figure 3.c.

It is important to note that, in linear second-order systems, assuming a monochromatic excitation torque, it is expected that the optimal switching law converges to solutions with no disconnection of the AMMR. This is because in second-order systems, the theoretical solution is well-known [14], and this behaviour, can be synthesised by the proposed hybrid control strategy. This assertion will be illustrated in the results of Section IV.

IV. WEC NUMERICAL EXAMPLE

This section analyses the three proposed controllers for the AMMR-based PTO, via numerical simulation. To that end, a second-order flap-based WEC model is used. Also, for clarity of exposition, $\tau_{ex}(t) = \sin(\phi t)$, is assumed. Accordingly, the parameters B_r and $J_{T,P}$, defined for a frequency $\phi = 2.6 rad/s$ (period of 2.4s), are presented in Table I. Also, to ease the comprehension of the results, the resulting WCB velocity is normalised with $2B_r$.

A. Sub-optimal continuous-time control evaluation

To evaluate the performance of the different controllers, comparisons with an ideal impedance-matching algorithm, are made. In Figure 4, the results of applying the sub-optimal controller from Section III-B can be appreciated. In Figure 4.a, the WCB velocity is shown, together with τ_{ex}. It can be noted, in Figures 4 a and b, that the extracted energy is below the 'ideal' case, i.e., from the results obtained using a PI impedance matching controller.

Employing this sub-optimal strategy is not straightforward. The selection of the commutation intervals is not simple, since depending on the clutching/declutching strategy, the controllability of the hybrid system can be compromised [9]. In the presented simulation, to resolve the appearance of undesired behaviour (such as uncontrolled switching), the commutation is forced to occur four times per period of the excitation torque, also guaranteeing velocity rectification.

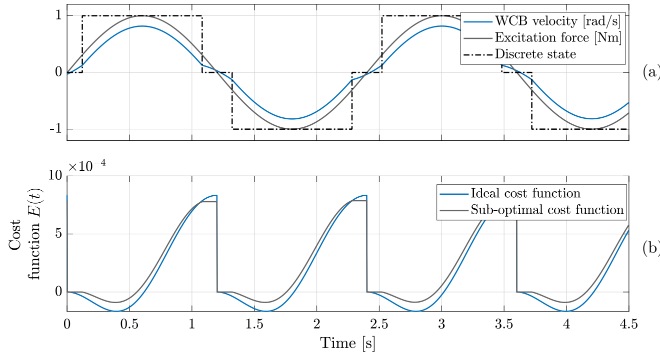

Fig. 4. Results of applying the sub-optimal continuous-time proposal. a) excitation torque, normalised WCB velocity and discrete states (q). b) Resulting cost function per interval, compared with the ideal.

B. Sub-optimal discrete-time (switching) control evaluation

Here, the sub-optimal control strategy, based on the procedure described in Subsection III-C, is presented and analysed. In this case, it is assumed that the generator controller is a linear PI, as illustrated in Figure 3.b. The parameters are adjusted as:

1) A sate-feedback controller with $K = [0, 70]$ is used (i.e., a proportional controller).
2) The time horizon $T = t_f - t_0$ is defined as half a period of the excitation torque. In this case, $T = 1.2s$.
3) Within T, the possibility of including three states ($N = 2$), beginning with $q = 1$, is evaluated.
4) The cost function $E(t)$ is iteratively computed. See, for instance, illustrative Figure 5. The 3D plot represents $E(t)$ as a function of the connection/disconnection instants.
5) The $[t_i\, t_{i+1}]$ that maximise $E(t)$ in each T are obtained. In Figure 5, t_1 represents the disconnection instance and t_2 the reconnection instance of the AMMR.

Remark 1: The selection $N = 2$ permits evaluating three discrete states in one half-period of the excitation force, which is, in practice, a realistic operation condition.

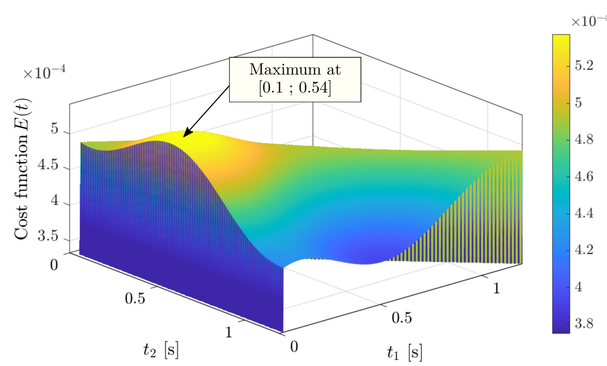

Fig. 5. Cost function evaluation in one half-period, as a function of the commutation instants.

The steady-state results of applying this strategy with $\phi = 2.62 rad/s$ can be appreciated in Figure 6. It can be noted that sub-optimal switching does not force the synchronisation of the excitation torque and the system velocity. However, these results might vary depending on the choice of the time horizon, controller parameters, and the number of switching instances.

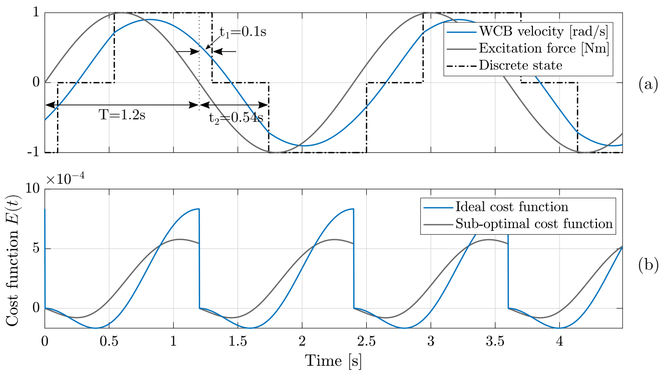

Fig. 6. Results of applying the sub-optimal discrete-time (switching) proposal. a) excitation torque, normalised WCB velocity and discrete states q. b) Resulting cost function per interval, compared with the ideal.

Also, it is important to mention that, the sub-optimal control structure from Subsection III-C, may provide results in which the generator is forced to cross zero velocity. This is not only detrimental to the operation of the generator but also forbids the AMMR from operating as a rectifier mechanism. However, as previously studied in [6] [7], a remarkable feature of the AMMR, is that it can be employed to increase mechanical power output, even using a simple proportional controller.

C. Global optimal control evaluation

In this subsection, the results of applying the global hybrid optimal control are analysed. It is worth mentioning that, with a monochromatic excitation torque, the optimal control from (10) converges to the results obtained with an adequately tuned PI, i.e., an impedance-matching controller. Indeed, observe Figure 7, where the transient behaviour of the system is plotted. Although, initially, switching is required, the solution converges to the no-declutching case, in which only the continuous-time optimal controller from (10) is employed.

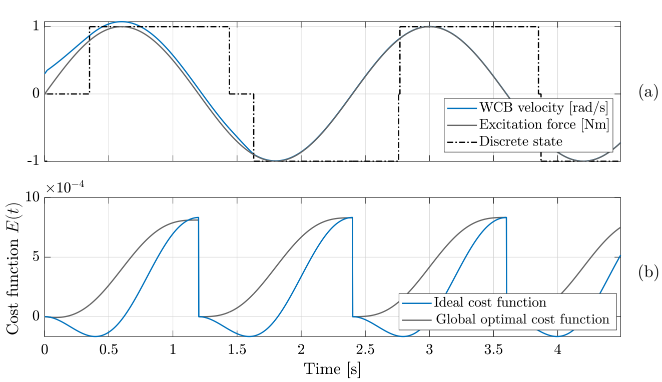

Fig. 7. Results of applying the global optimal proposal. a) excitation torque, normalised WCB velocity and discrete states (q). b) Resulting cost function per interval, compared with the maximum theoretical.

V. CONCLUSIONS

AMMR technology represents a compelling pathway to address traditional rotary-generator-based PTO drawbacks. However, it also poses interesting problems to the design of a suitable control algorithm. In this PTO structure, not only the generator torque, but also the clutching and declutching events, may be employed as a control action in the system, to maximise energy extraction.

To solve the optimal control problem, it was proven that, assuming a second-order system, the selection of the switching interval and the design of a control algorithm, can be separately tackled. Consequently, three different control proposals were formulated: Two sub-optimal proposals, in which one control structure is fixed, and a global optimal solution.

Finally, aiming to illustrate the results obtained with the proposed methods, a numerical example was presented. Although preliminary, the proposal presented in this work paves the way for future control development for the AMMR-based WEC. In this context, the analysis and results serve as the foundation for designing an autonomous control algorithm in more complex scenarios, considering system constraints, non-frequency dependent models, and including the effects of τ_{ex} estimation, among some of the challenges that remain to be addressed.

REFERENCES

[1] J. V. Ringwood, S. Zhan, and N. Faedo, "Empowering wave energy with control technology: Possibilities and pitfalls," *Annual Reviews in Control*, vol. 55, pp. 18–44, 2023.

[2] B. Guo and J. V. Ringwood, "A review of wave energy technology from a research and commercial perspective," *IET Renewable Power Generation*, vol. 15, no. 14, pp. 3065–3090, 2021.

[3] H. A. Said and J. V. Ringwood, "Grid integration aspects of wave energy—overview and perspectives," *IET Renewable Power Generation*, vol. 15, no. 14, pp. 3045–3064, may 2021.

[4] R. Ahamed, K. McKee, and I. Howard, "Advancements of wave energy converters based on power take-off (PTO) systems: A review," *Ocean Engineering*, vol. 204, p. 107248, may 2020.

[5] X. Li, D. Martin, C. Liang, C. Chen, R. G. Parker, and L. Zuo, "Characterization and verification of a two-body wave energy converter with a novel PTO," *Renewable Energy*, vol. 163, pp. 910–920, jan 2021.

[6] L. Yang, J. Huang, N. Congpuong, S. Chen, J. Mi, G. Bacelli, and L. Zuo, "Control co-design and characterization of a power takeoff for wave energy conversion based on active mechanical motion rectification," *IFAC-PapersOnLine*, vol. 54, no. 20, pp. 198–203, 2021.

[7] L. Yang, J. Huang, J. Mi, M. Hajj, G. Bacelli, and L. Zuo, "Optimal power analysis of a wave energy converter with a controllable power takeoff based on active motion rectification," *IFAC-PapersOnLine*, vol. 55, no. 27, pp. 299–304, 2022.

[8] P. Fornaro and J. V. Ringwood, "Stability analysis of an active mechanical motion rectifier for wave energy conversion systems," in *XX Workshop on Sig. Proc. and Control - RPIC, Argentina*, 2023.

[9] P. Fornaro and J. V. Ringwood, "On the controllability of an active mechanical motion rectifier for wave energy converters," in *2024 American Control Conference, Toronto, Canada*, 2024.

[10] F. Lin, L. Y. Wang, W. Chen, and M. P. Polis, "On controllability of hybrid systems," *IEEE Tran. on Aut. Control*, vol. 66, no. 7, 2021.

[11] G. Labinaz, M. M. Bayoumi, and K. Rudie, "A survey of modeling and control of hybrid systems," *Annual Reviews in Control*, 1997.

[12] J. Falnes, *Ocean Waves and Oscillating Systems*. Cambridge University Press, 2002.

[13] W. Bencze and G. Franklin, "A separation principle for hybrid control system design," *IEEE Control Systems*, vol. 15, no. 2, 1995.

[14] Y. Pena-Sanchez, C. Windt, J. Davidson, and J. V. Ringwood, "A critical comparison of excitation force estimators for wave-energy devices," *IEEE Tran. on Control Syst. Tech.*, vol. 28, no. 6, 2020.